PHYSICAL REVIEW B VOLUME 62, NUMBER 12 15 SEPTEMBER 2000-II

Real-space, real-time method for the dielectric function

G. F. Bertsch,[1,*] J.-I. Iwata,[2] Angel Rubio,[3,†] and K. Yabana[2,‡]

[1]*Department of Physics and National Institute for Nuclear Theory, University of Washington, Seattle, Washington 98195*

[2]*Institute of Physics, University of Tsukuba, Tsukuba 305-8571, Japan*

[3]*Departamento de Física Teórica, Universidad de Valladolid, Valladolid and Donostia International Physics Center, San Sebastian, Spain*

(Received 8 June 2000)

We present an algorithm to calculate the linear response of periodic systems in the time-dependent density functional theory, using a real-space representation of the electron wave functions and calculating the dynamics in real time. The real-space formulation increases the efficiency for calculating the interaction, and the real-time treatment decreases storage requirements and allows the entire frequency-dependent dielectric function to be calculated at once. We give as examples the dielectric functions of a simple metal, lithium, and an elemental insulator, diamond.

I. INTRODUCTION

Real-space methods have proven their utility in calculating the linear response of finite systems in time-dependent density functional theory.[1,2] However, there has been the perception that real-space methods are unsuitable for infinite periodic systems. The problem is that the long range polarization currents are important but are dynamically independent of the local state of the electrons within the unit cell. Stated differently, the polarization gives rise to a surface charge at the surface of any finite sample, but the resulting electric field is independent of the charge density within any cell in the interior. The necessity to introduce the polarization as an independent degree of freedom has been well recognized in the literature of the density functional theory.[3–6]

We will show here that in fact it is straightforward to treat infinite systems in the real-time formulation of time-dependent density functional theory, simply by adding as one additional dynamic variable the surface charge. Formally, this is conveniently done adding a gauge field within a Lagrangian. A gauge formalism has also been very recently applied by Kootskra *et al.*,[7] however using a frequency representation rather than solving real-time equations. In our formulation, we derive the dynamic equations from the Lagrangian:

$$L=\int_\Omega d^3r\Bigg(\frac{\sum_i |\vec\nabla\phi_i/i-eA\hat z\phi_i|^2}{2m}-\frac{1}{8\pi}\vec\nabla V(\mathbf r)\cdot\vec\nabla V(\mathbf r)+en(\mathbf r)V(\mathbf r)+en_{\rm ion}(\mathbf r)V(\mathbf r)+\mathcal V_{xc}[n(\mathbf r)]+\mathcal V_{\rm ion}[\rho(\mathbf r,\mathbf r')]\Bigg)-\frac{\Omega}{8\pi}\left(\frac{dA}{dt}\right)^2-i\int_\Omega d^3r\sum_i\phi_i^*\frac{\partial\phi_i}{\partial t}. \tag{1}$$

Here the ϕ_i are the Bloch wave functions of the electrons, normalized so that $n(\mathbf r)=\Sigma_i|\phi_i(\mathbf r)|^2$ is the electron density. The volume of the unit cell is Ω. The electromagnetic interaction is separated into a Coulomb field $V(\mathbf r)$ that satisfies periodic boundary conditions in the unit cell and a vector gauge field $\hat z A(t)$. Note that the gauge field is uniform, without any dependence on $\mathbf r$. The electric field is then given by

$$\vec{\mathcal E}=-\vec\nabla V-\hat z\frac{dA}{dt}.$$

In these formal equations, we use units with $\hbar=c=1$.

The other pieces of the first integral are the usual terms in the Kohn-Sham energy functional. The term $en(\mathbf r)V(\mathbf r)$ gives the direct Coulomb interaction of the electrons, except for the surface charging. The ionic interaction is separated into a long-range part that can be associated with an ionic charge density $n_{\rm ion}(\mathbf r)$ and a short-range part $\mathcal V_{\rm ion}$. The separation is somewhat arbitrary, but is useful because the periodicity of V then takes the ionic lattice into account automatically. The latter depends on the orbital angular momentum of the electrons in typical *ab initio* pseudopotentials. It therefore depends on the full one-electron density matrix $\rho(\mathbf r,\mathbf r')=\Sigma_i\phi_i^*(\mathbf r)\phi_i(\mathbf r')$. We have emphasized this point because nonlocal interactions do not respect gauge invariance. The invariance is of course restored if the density matrix is gauged. This will be described in more detail below. Finally, the $\mathcal V_{xc}$ is the usual exchange-correlation energy density of density functional theory.

Requiring the Lagrangian action to be stationary gives equations of motion for ϕ_i and A and the Poisson equation for V. The dynamic equation for ϕ_i is the time-dependent Kohn-Sham equation,

$$-\frac{\nabla^2}{2m}\phi_i-\frac{e}{mi}A\nabla_z\phi_i+\frac{e^2}{2m}A^2\phi_i+\left(eV+\frac{\delta\mathcal V_{\rm ion}}{\delta n}+\frac{\delta\mathcal V_{xc}}{\delta n}\right)\phi_i=i\frac{\partial}{\partial t}\phi_i. \tag{2}$$

The equation for A is

$$\frac{\Omega}{4\pi}\frac{d^2A}{dt^2}-\frac{e}{m}\sum_i\langle\phi_i|\nabla_z/i|\phi_i\rangle+\frac{e^2}{m}AN_e+\frac{\delta}{\delta A}\int_\Omega\mathcal V_{\rm ion}d^3r=0, \tag{3}$$

0163-1829/2000/62(12)/7998(5)/$15.00

where $N_e = \int_\Omega d^3 r n(\mathbf{r})$ is the number of electrons per unit cell.

II. LINEAR RESPONSE, SUM RULE AND SIMPLE MODELS

The calculation of the dielectric function using the above real-time dynamic equations is very similar to the corresponding calculation of dynamic polarizability of finite systems.[2] We first solve the static equations (with $A=0$) to get the ground-state electron orbitals and the periodic Coulomb potential V. The system is then perturbed by making a sudden change in A, $A(t=0_+)=A_0$. This corresponds to applying a short duration electric field at $t=0$, $\mathcal{E}(t) = -A_0\delta(t)$. In the linear response regime, the perturbed system contains all the excitations in proportion to their excitation strength. One can then determine the entire frequency dependence response in a single time-dependent calculation, which would not be the case if the system were perturbed in the usual way with an oscillatory external field. From the time-dependent evolution, we find the polarization electric field $\mathcal{E}(t) = -dA(t)/dt$, corresponding to a surface charge density $\sigma(t) = dA(t)/4\pi dt$. The dielectric function $\epsilon(\omega)$ is just the ratio of the Fourier components of the external and the total fields; it is given by

$$\frac{1}{\epsilon(\omega)} - 1 = \frac{1}{A_0}\int_{0_+}^{\infty} e^{i\omega t - \eta t}\frac{dA(t)}{dt}dt. \tag{4}$$

Here η is a small quantity to establish the imaginary part of the response. In principle the resulting theory automatically respects the Kramers-Kronig relation.

The linear energy-weighted sum rule is easily derived in this formalism. The sum rule may be expressed as[9]

$$\int_0^\infty \omega \,\mathrm{Im}\,\epsilon^{-1}(\omega)\,d\omega = -\frac{2\pi^2 e^2 N_e}{m\Omega}. \tag{5}$$

To calculate the sum rule with our Lagrangian, we write the integral using Eq. (4)

$$\int_0^\infty \omega \,\mathrm{Im}\,\epsilon^{-1}(\omega)\,d\omega = \frac{1}{A_0}\int_0^\infty dt\,\frac{dA}{dt}\,\mathrm{Im}\int_0^\infty d\omega\,\omega e^{i\omega t - \eta t}$$

$$= \frac{\pi}{2A_0}\left(\frac{d^2A}{dt^2}\right)_{t=0_+}. \tag{6}$$

The second derivative in the last expression is obtained from Eq. (3). At $t=0_+$, the wave functions have not yet had time to change, $A(0_+)=A_0$ and $\langle\nabla_z\rangle = 0$. Then if the last term in Eq. (3) can be neglected,

$$\frac{d^2A}{dt^2} = -\frac{4\pi e^2 N_e A_0}{m\Omega} \tag{7}$$

and Eq. (5) follows immediately. Thus the time-dependent treatment satisfies the sum rules automatically to the extent permitted by the last term. That term is only nonzero for nonlocal pseudopotentials, and in fact it may improve the accuracy of the theory by incorporating effects of the core electrons on the dynamic properties.[8]

Let us now see how the gauge field treatment works in a simple analytically solvable model, namely the electron gas. As mentioned before, when the field A_0 is applied, there is no immediate response to the operator ∇, since the wave function does not change instantaneously. However, in the Fermi gas, the single-particle states are eigenstates of momentum so the response remains $\langle\nabla\rangle = 0$ for all time. Putting this in Eq. (3), and dropping the pseudopotential term, the equation for A becomes simple harmonic motion, with the solution

$$A(t) = A_0 \cos \omega_{pl} t, \tag{8}$$

where ω_{pl} is the plasmon frequency,

$$\omega_{pl}^2 = \frac{4\pi e^2 N_e}{m\Omega} = \frac{4\pi e^2 n}{m}. \tag{9}$$

The dielectric function may now be calculated from the time integral Eq. (4). One obtains the familiar electron gas result,

$$\epsilon(\omega) = 1 - \frac{\omega_{pl}^2}{\omega^2}. \tag{10}$$

One sees that the derivation here is much simpler than the usual one using the Coulomb gauge. There one formulates the response in a particle-hole representation, and takes the external field to be of the form $e^{iq\cdot r}$ with q finite. The dielectric function is then found by taking the $q\to 0$ limit.

We can make another simple model for the opposite extreme of a tightly bound electron in the unit cell. Assume that the ion potential $eV_{\mathrm{ion}}(\mathbf{r}) + \delta\mathcal{V}_{\mathrm{ion}}/\delta n$ can be approximated by a harmonic oscillator potential in the region over which the electron wave function is appreciable. According to Kohn's theorem,[10] the response is just the same as for an isolated electron in the same ionic potential. This comes out of Eqs. (2) and (3) in the following way. The initial impulse A_0 starts the electron moving, and as a result both $V(\mathbf{r})$ and $\delta\mathcal{V}_{xc}/\delta n(\mathbf{r})$ become time-dependent. Together with the changing A, the electron in the unit cell drags its self-induced field with it, and the accelerations associated with these three terms in Eq. (2) exactly cancel. The remaining ionic terms then produce simple harmonic motion for ϕ.

III. NUMERICAL DETAILS

The computational algorithm we employ is identical to the ones we used for clusters and molecules, which was based on a method introduced in nuclear physics.[11] The Kohn-Sham operator is represented on a real space grid as in Ref. 12. There are a number of technical details associated with the periodicity and with the gauge potential that did not arise for the finite-system calculations. In the new code, the potential $V(\mathbf{r})$ is calculated by Fourier transformation of the Poisson equation rather than a relaxation method. This gives automatically the required periodicity to $V(\mathbf{r})$. The wave functions ϕ_i represent Bloch states of the periodic lattice, and they are constructed with the corresponding periodic boundary conditions labeled by the Bloch momenta k. The periodic boundary condition on the Bloch wave function $\phi_k(r+a) = \exp(iak)\phi_k(\mathbf{r})$ is easily implemented in the relaxation method used to find eigenstates. In practice, many

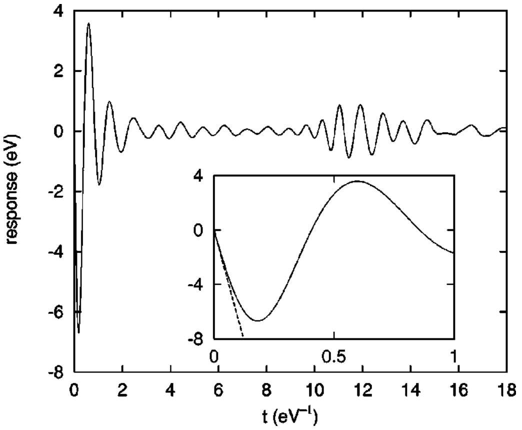

FIG. 1. The induced polarization field $(1/A_0)dA/dt$ in lithium metal is shown as a function of time (solid). In this calculation, the occupied states were represented by points on a 16^3 mesh in *k*-space. The dashed line show the early-time behavior required by the sum rule.

Bloch states are needed to obtain smooth dielectric functions. However, constructing the states takes much less time than for the same number of electrons in a finite system, because the Bloch states in a given band are automatically orthogonal.

We use here the same energy density functional that we used previously for finite systems. Only the valence electrons are included explicitly; core electrons are treated by a pseudopotential.[13,14] The exchange-correlation energy of the electrons is calculated in the local density approximation following the prescription of Ref. 15.

The presence of a vector gauge potential requires a modification in the pseudopotential calculation, as indicated in the introduction. In particular, the A-dependence of the $\mathcal{V}_{\rm ion}$ term in Eq. (2) must be consistent with the last term in Eq. (3) in order to have the algorithm conserve energy. We implement the A-dependence of $\mathcal{V}_{\rm ion}$ simply by gauging the density matrix directly,

$$\mathcal{V}_{{\rm ion},A}(\rho(\mathbf{r},\mathbf{r}'))=\mathcal{V}_{\rm ion}(e^{iA(z-z')}\rho(\mathbf{r},\mathbf{r}')).$$

As in the finite systems calculations, energy is conserved to a very high accuracy with the algorithm,[11] provided the time step is less than the inverse energy span of the Kohn-Sham operator.

IV. LITHIUM

In this section we demonstrate the feasibility of the method with lithium as an example of a simple metal. As other alkali metals, lithium has a Fermi surface which is nearly spherical. However, unlike sodium and potassium, the effective mass of the electrons at the Fermi surface is significantly enhanced over the free-Fermi gas value ($m^*\approx 1.6m_e$).

The Kohn-Sham operator is represented in coordinate space with a uniform spatial mesh. The lattice spacing of the bcc unit cell of Li metal is $a=3.49$ Å, and we take a mesh spacing of $\Delta x=0.58$ to subdivide the cell into a 6^3 lattice of mesh points. We use a time step of $\Delta t=0.01\,{\rm eV}^{-1}$ which is sufficient to conserve energy to 10^{-4} eV over the time integration interval, $T=18\,{\rm eV}^{-1}$.

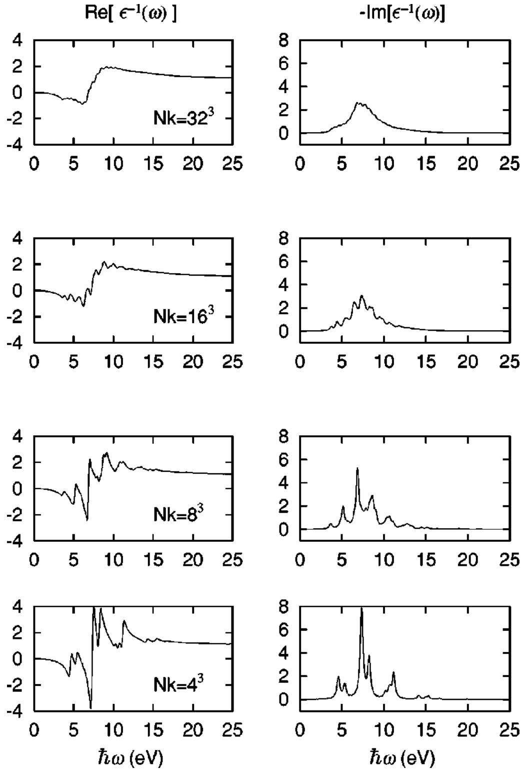

FIG. 2. Real and imaginary parts of the inverse dielectric function in lithium, shown for various meshes on the Brillouin zone.

We sample the occupied states with a uniform mesh in momentum space. With a finite set of occupied orbitals, the allowed excitation energies will be discrete, and the metallic behavior, $\epsilon(\omega)\rightarrow\infty$, is only reached in the limit of an infinitely dense momentum space lattice. However, it is our view that the TDLDA loses validity at long times when other degrees of freedom can be excited. This is the case for the low frequency response of metals, where the imaginary part of the dielectric responses is dominated by phonons and inelastic electron scattering.

In Fig. 1 we show the normalized time-dependent polarization field, $A_0^{-1}dA/dt$ over the time interval $t=[0,18]\,{\rm eV}^{-1}$. The inset shows an expanded view of the initial response in the interval $[0,1]\,{\rm eV}^{-1}$. The dashed line is the comparison with the linear behavior deduced from the sum rule, $A_0^{-1}dA/dt=-4\pi e^2N_et/m\Omega$. The agreement shows that the local sum rule is nearly satisfied, despite the fairly large optical effective mass.

In Fig. 2 we show the inverse dielectric function computed from Eq. (4) for various meshes in the Brillouin zone. We employ $\eta=0.2$ eV to smooth the response in the Fourier transformation. We see that the response becomes smoother, the more finely the Fermi sea is sampled. With a 32^3 lattice of Bloch states, we get results smooth enough to be compared with measurement.

In Fig. 3 we show the real and imaginary parts of the inverse dielectric function in the frequency interval $0-20\,{\rm eV}/\hbar$. The dashed lines show the empirical function from Ref. 16. There is also another theoretical calculation in the literature.[17] The agreement is quite good, especially con-

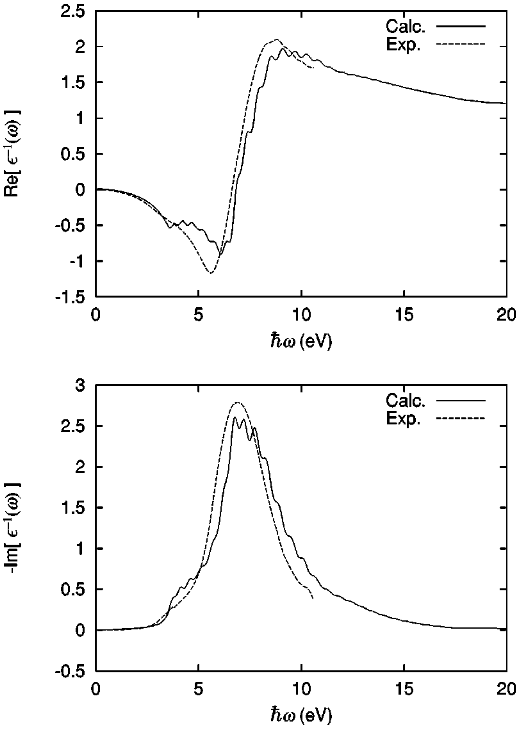

FIG. 3. Real and imaginary parts of the response $\epsilon^{-1}(\omega)$ as a function of frequency. Here the orbitals of the valence band were presented by Bloch states on a 32^3 mesh in *k*-space. The empirical response from Ref. 16 is shown with the dashed lines.

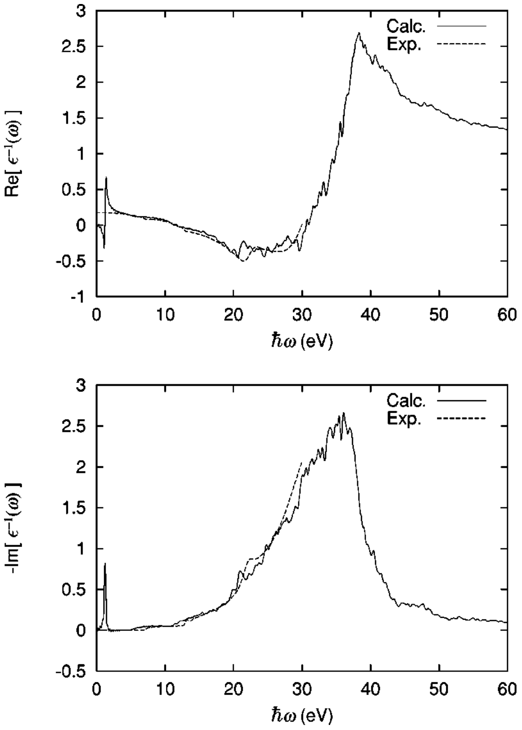

FIG. 4. Real and imaginary parts of the response $\epsilon^{-1}(\omega)$ for diamond. Here the orbitals of the valence band were represented by Bloch states on a 16^3 mesh in *k*-space.

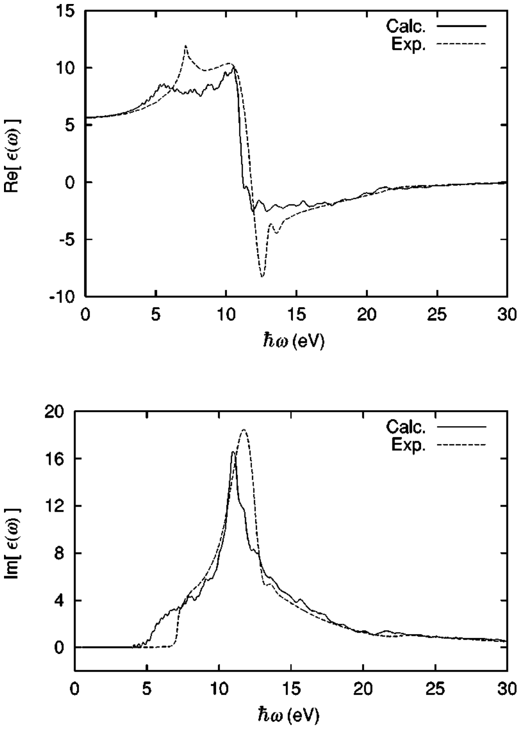

FIG. 5. Real and imaginary parts of the dielectric function $\epsilon(\omega)$ for diamond. The spurious plasmon has been excluded by using the Kramers-Kronig relation to determine the real part of the dielectric function, integrating over the imaginary response from 4 eV. The dashed curve shows the experimental dielectric function, taken from Ref. 16.

sidering that the calculation is *ab initio* with an energy density functional that much simpler than more recent ones. The main feature in the absorptive response is the plasmon at 7 eV and its width. The peak position is significantly downshift from the naive plasmon frequency, $\omega_{pl}=\sqrt{4\pi e^2 n/m} \approx 8$ eV. The width is associated with interband transitions and is also well reproduced.

V. DIAMOND

In this section we compute the dielectric response of a typical elemental insulator, diamond. The diamond lattice is represented in our calculation by the conventional unit cell which contains 8 carbon atoms. The wave functions of the four valence electrons of each carbon are calculated explicitly in Eq. (2) while the core electrons are only treated implicitly by the pseudopotential. We found in earlier studies of carbon structures that the Kohn-Sham Hamiltonian requires a mesh spacing $\Delta x = 0.3$ Å to get orbital energies to an accuracy of 0.1 eV; in the calculation here we take a 12^3 lattice in the unit cell which implies $\Delta x = 3.56/12$ Å $= 0.297$ Å. With a smaller mesh spacing than for lithium, the span the Kohn-Sham operator is increased and the time step Δt must be reduced accordingly. We use here $\Delta t = 0.002\ \mathrm{eV}^{-1}$.

With a cubical unit cell and 8 carbon atoms, there are $8 \times 4/2 = 16$ occupied bands. The bands are actually two-fold degenerate because we have not exploited the symmetry that allows a smaller unit cell with two carbons. In each band we take a lattice of up to 16^3 points to represent the Bloch states.

For an insulator, a reference point of the vector potential $A(t)$ should be irrelevant. However, in our numerical implementation of the equations, we found that at the energy of the static solution has a still dependence on A. This gives rise to a spurious low frequency mode of oscillation.

This may be seen in the plots of the response in Fig. 4. The spurious adiabatic evolution gives an unphysical plasmon at ≈ 1.2 eV, which dominates the dielectric response at lower frequencies. Though the amount of strength associated with this spurious plasmon is very small, 0.007 electrons out of the total of 32, it has a qualitative effect on the response at very low frequency. The frequency and strength decrease the finer the spatial mesh, showing that it is an artifact of the discrete mesh representation of the coordinate space.

To infer the dielectric function near $\omega=0$, we apply the Kramers-Kronig relation to the imaginary part of the response, but excluding the spurious plasmon peak. This gives the predicted dielectric function shown in Fig. 5. The empirical dielectric function is shown as the dashed line. The agreement is good, as indeed was found solving the TDLDA equations by other methods,[18] but one can also see the effect of the well-known shortcoming of TDLDA, that the predicted band gaps are too small.[19,20] The theoretical absorption strength become significant starting at about 5 eV excitation, while the empirical absorption begins at around 7 eV. Nevertheless, the dielectric constant comes out in good agreement with the empirical,[18] being within a percent of the empirical value of $\epsilon(0)=5.67$.

VI. CONCLUSIONS

We see that the method not only works in principle, but produces fairly accurate dielectric functions in the cases of a simple metal and a simple insulator. In lithium, the theory describes the metallicity as well as the interband transitions. In diamond, there is a spurious plasmon at low frequency due to the discrete mesh representation in coordinate and momentum spaces. However, it can be easily dealt with and then the dielectric function has an excellent quality except for a small band gap region. We find that two benefits of the real-space, real-time formulation of the TDLDA in finite systems[21] are preserved in our implementation here. The real-space method allows the Kohn-Sham operator and electron-electron interactions to be evaluated efficiently.[12] Computational efficiency is also gained by calculating the response in real time in that all frequencies are calculated at once. Finally, the method requires much less storage than methods using a particle-hole representation of the time-varying wave function.

ACKNOWLEDGMENTS

We acknowledge discussions with E.K.U. Gross, R. Martin, J. Rehr, and R. Resta. This work was supported in part by the Department of Energy under Grant No. DE-FG03-00-ER41132, by the DGES (Grant No. PB98-0345) and by the JCyL (Grant No. VA28/99), and by the Ministry of Education, Science and Culture, Japan, Contract No. 11640372. J.I. and K.Y. acknowledge the Institute of Solid State Physics, University of Tokyo, and the Research Center for Nuclear Physics, Osaka University, for their use of supercomputers. A.R. acknowledges the hospitalty of the Institute for Nuclear Theory where this work was started and computer time provided by the Center de Coputació i Comunicacions de Catalunya.

---

*Email address: bertsch@phys.washington.edu
†Email address: arubio@mileto.fam.cie.uva.es
‡Email address: yabana@nucl.ph.tsukuba.ac.jp

[1] I. Vasiliev, S. Ogut, and J.R. Chelikowsky, Phys. Rev. Lett. **82**, 1919 (1999).

[2] K. Yabana and G.F. Bertsch, Phys. Rev. B **54**, 4484 (1996).

[3] R. Resta, Rev. Mod. Phys. **66**, 899 (1994).

[4] X. Gonze, P. Ghosez, and R.W. Godby, Phys. Rev. Lett. **74**, 4035 (1995).

[5] G. Ortiz, I. Souza, and R.M. Martin, Phys. Rev. Lett. **80**, 353 (1998).

[6] R. Resta, Int. J. Quantum Chem. **75**, 599 (1999).

[7] F. Kootstra, P.L. de Boeij, and J.G. Snijders, J. Chem. Phys. **112**, 6517 (2000).

[8] For a study of nonlocal pseudopotential effects on oscillator strength, see K. Yabana and G.F. Bertsch, Phys. Rev. A **58**, 2604 (1998).

[9] G.D. Mahan, *Many-Particle Physics* (Plenum, New York, 1981), Eq. (5.7.4).

[10] J.F. Dobson, Phys. Rev. Lett. **73**, 2244 (1994).

[11] H. Flocard, S. Koonin, and M. Weiss, Phys. Rev. C **17**, 1682 (1978).

[12] J. Chelikowsky, N. Troullier, K. Wu, and Y. Saad, Phys. Rev. B **50**, 11 355 (1994).

[13] N. Troullier and J.L. Martins, Phys. Rev. B **43**, 1993 (1991).

[14] L. Kleinman and D. Bylander, Phys. Rev. Lett. **48**, 1425 (1982).

[15] J. Perdew and A. Zunger, Phys. Rev. B **23**, 5048 (1981).

[16] *CRC Handbook of Chemistry and Physics* (CRC Press, Boca Raton, 77th ed., 1996), pp. 12–133.

[17] H. Bross and M. Ehrnsperger, Z. Phys. B: Condens. Matter **97**, 12 (1995).

[18] V.I. Gavrilenko and F. Bechstedt, Phys. Rev. B **55**, 4343 (1997).

[19] M.S. Hybertsen and S.G. Louie, Phys. Rev. B **34**, 5390 (1986).

[20] R.W. Godby, M. Schlueter, and L.J. Sham, Phys. Rev. B **37**, 10 159 (1988).

[21] G.F. Bertsch, A. Rubio, and K. Yabana, Los Alamos preprint physics/0003090 (to be published).